Gazi Mühendislik Bilimleri Dergisi
2017, 3(2): 1-14

http://gmbd.gazipublishing.com/

Guidance and Control of a Quadrotor towards a Moving Land Platform

Bülent Özkan[a*]

[a] *TÜBİTAK Defense Industries Research and Development Institute, ANKARA 06261, TURKEY*

ARTICLE INFO

Received: 05.05.2017
Accepted: 12.08.2017

Keywords:
Guidance and control, quadrotor, linear homing guidance law, two-stage control system, moving platform

Corresponding Authors
e-mail: bulent.ozkan@tubitak.gov.tr

ABSTRACT

Quadrotors are utilized in several military and civil applications. To improve the performance characteristics, their weight is desired to be kept at minimum. However, the battery which constitutes one of the major components of a quadrotor weighs more if its range is extended. When a moving destination point is considered as well, the power requirement becomes larger. Thus, a proper motion planning comes into the picture as a necessity for the quadrotor to reduce the total operation time and hence to lower the power consumption. In this study, a novel guidance-based motion planning scheme is proposed regarding two different guidance laws towards a moving land platform. Moreover, an effective two-stage control system is designed in a way compatible with the suggested guidance laws. The success of the constructed guidance and control algorithm is demonstrated by means of suitable computer simulations. Eventually, it is concluded that the linear homing guidance law leads to more satisfactory results than the other guidance approach utilized in this study, i.e. body pursuit guidance law.

Dört Döner Kanatlı Bir Sistemin Hareketli Bir Kara Platformuna Doğru Güdüm ve Denetimi

MAKALE BİLGİSİ

Alınma: 05.05.2017
Kabul: 15.08.2017

Anahtar Kelimeler:
Güdüm ve denetim, dört döner kanatlı sistem, doğrusal hedef takibi güdüm kuralı, iki kademeli denetim sistemi, hareketli platform

Sorumlu Yazar
e-mail: bulent.ozkan@tubitak.gov.tr

ÖZET

Dört döner kanatlı sistemler (DDKSs), askerî ve sivil alanda çeşitli uygulamalarda kullanılmaktadır. Belirtilen sistemlerin başarımlarını (performanslarını) yükseltmek için, toplam kütleleri asgarî düzeyde tutulmalıdır. Öte yandan, menzil gereksinimindeki büyüme, DDKS'lerin kritik bileşenlerinden olan güç kaynağının kütlesini de artıracaktır. Ayrıca, hareketli hedef noktası söz konusu olduğunda güç gereksinimi de fazlalaşacaktır. Bu nedenle, toplam işletim süresinin kısaltılması ve dolayısıyla güç tüketiminin aşağıya çekilebilmesi adına, DDKS'lerin hareket planlamasının uygun bir şekilde yapılması önem arz etmektedir. Bu çalışmada, ele alınan bir DDKS'nin hareketli bir yer platformuna yönlendirilmesinde uygulanabilecek güdüm esaslı farklı bir hareket planlaması yaklaşımı önerilmektedir. Belirtilen yöntemde iki farklı güdüm kuralı göz önüne alınmış olup, bu kurallarla uyumlu olacak şekilde iki kademeli etkin bir denetim sistemi de tasarlanmıştır. Oluşturulan güdüm ve denetim algoritmasının başarımı, uygun şekilde kurgulanmış bilgisayar benzetimleri yardımıyla gösterilmeye çalışılmıştır. Sonuç olarak, doğrusal hedef takibi güdüm kuralının ele alındığı durumlarda, gövde takibi güdüm kuralının uygulandığı senaryolara nazaran daha tatminkâr sonuçların elde edildiği gözlenmiştir.

1. Introduction

Quadrotors which involve four identical propellers driven by rotors have become very popular in recent years in several fields. Especially in reconnaissance and rescue works, they are preferred to helicopters because of their relatively simple rotor mechanics, linear flight mechanics, high maneuvering capability, vertical take-off and landing property, and smaller propellers compared to the single-propeller system rotors (1-6). Also, their advantage on flying at relatively low altitudes and hovering over rough terrains has attracted a great amount of attention (7). The simple rotor mechanics of quadrotors are provided by the configuration which include four identical propellers put at a cross-form. Also, the fact that the left and right propellers have rotations in clockwise sense while the front and rear ones rotate in the counter-clockwise direction as shown in Fig. 1 leads the gyroscopical effects on the system and aerodynamical torques on nominal flight conditions to almost nullify. The effect of the aerodynamical force and moment components on the system can be ignored especially at lower speeds. This provides quadrotors with having more linear dynamic behaviour compared to their single-propeller counterparts. Furthermore, less kinetic energy is stored in quadrotors during flight thanks to their smaller rotors and thus the risk of harming the environment and living creatures around is considerably minimized under the circumstances like colliding a substance [1-5] .

In order to reach better performance characteristics, quadrotors are desired to be made as light as possible. However, the actuators, i.e. direct current (DC) electric motors combined of a rotor and stator, driving electronic cards, camera used to acquire the surrounding and target information, and battery cause the total weight of a quadrotor to increase as they are mounted on its main chassis. When the range of the quadrotor is extended, its total power requirement grows and hence the size and weight of the battery become larger, too. For this reason, an efficient motion planning of the quadrotor gains more importance to allow less power consumption [2]. Since almost all of the quadrotor studies handle stationary, or fixed, destination points, the corresponding motion planning is made in accordance with some certain polynomial fits [8]. Moreover, the path planning approaches dealing with certain mapping and searching algorithms are seen with the support of vision-based navigation and Kalman filters in the literature [9-11]. The laser-based guidance arises as an alternative motion planning manner for the quadrotors as well [12]. In this scene, most of the effort is spent to optimize the trajectory of the quadrotor with respect to certain criteria such as minimum time and/or the shortest path [13-14]. As a study conducted in a similar manner with the present work, a quadrotor is guided towards the predefined moving target by keeping the heading of the quadrotor unchanged. Unlike the present work, the four control variables are chosen to be angular position, or attitude variables, and height of the quadrotor in this study [15].

Once the motion of the quadrotor is planned against a specified destination point, the forthcoming task is to design an appropriate control system to realize the commands generated by the motion planning algorithm. In this sense, the major challenge of quadrotors comes into the picture: the underactuation. That means the quadrotor posseses only four degrees of freedom because of its four propellers as the inputs while it needs at least six degrees of freedom to be able to reach a specific location in the space without any deficiency [4]. While some specific control algortihms are established to resolve the underactuation problem such as backstepping control method, the usual tendency is to designate the control variables at a number which is not greater than four [16]. In this sense, some of the quadrotors are developed so as to keep them at a specified height from the ground. That is, only altitude control problem is dealt with by releasing the other five degrees of freedom4. In this scene, the hovering motion appears as a specific case of the altitude control problem [6]. The hovering control problem of the quadrotors is handled under parameter uncertainties and well-suited robust control algorithms are developed such as adaptive backstepping control [11]. Besides, the attitude control of the quadrotors is examined in some of the works. In this approach, the angular position variables, or Euler angles, of the quadrotors are aimed to be stabilized [8]. For the attitude control of the quadrotors, robust control methods including sliding mode control and backstepping methods are considered both theoretically and experimentally as well as the classical approaches [18; 23]. Apart from those, there are studies making the control of four selected degrees of freedom of the quadrotors in the literature. In general, those four degree of freedoms are gathered as a mixture of translational and rotational motion components about selected axes by leaving two axes of the quadrotor uncontrolled. For such kind of control purposes, two-stage control algorithms are also established by accounting the linear position or velocity and angular position variables separately as an alternative to single-stage control schemes [38; 2; 15; 39; 42]. In fact, since the

PRINT ISSN: 2149-4916 E-ISSN: 2149-9373

translational motion variables are dependent on the rotational variables, such kind of a two-stage control scheme is necessary when at least one of the translational variable of the quadrotor is intended to be controlled as well as the three rotational variables [8; 4]. The two-stage control concept is also used for both tracking and stabilization purposes by designing the outer and inner loops for tracking and stabilization, respectively [28; 35; 13]. In these control systems, robust control methods such as norm-based approaches, backstepping, and sliding mode control are considered in addition to the gain scheduling approach and the most frequently-used classical PID (proportional plus integral plus derivative) control action [29; 24; 4; 40; 30; 25; 17]. Fuzzy PID-type control schemes are applied to quadrotors for vertical take-off and landing purpose as well [1]. In this extent, the application of a linear quadratic regulator is also examined along with a suitable trajectory optimization [9] Regarding the parameter uncertainties in the modeling, adaptive control schemes are proposed for the quadrotors [12]. In order to make the performance characteristics of a quadrotor considered approach a reference quadrotor model, an automatic regulation process is constructed upon the adjustment of the controller parameters for different load conditions [36]. Also, studies conducted on the control of the quadrotors with fuzzy logic are encountered in the literature [14].

In this study, the motion planning and control of a quadrotor which is intended to carry a payload from a stationary initial point to a prescribed moving land platform at a moderate distance for either military or civil purpose are investigated. Namely, the payload can be munition, food or first aid material. Since the moving platform specified as the target is assumed to be far away from the initial point, it is desired for the quadrotor to catch it within the shortest time duration possible and consume the power at a minimum level. Keeping this motivation, the motion planning of the quadrotor against a moving platform is tried to be made according to the guidance concept which is extensively applied to guided munitions and rarely to robotic arms [38; 31; 41]. Actually, this “guidance” approach is a way different from the landing problem of quadrotors on a moving platform by the assistance of optical flow geometry [21]. As the primary contribution of this study, the guidance algorithm is built with respect to two different approaches: The selected quadrotor is guided towards the moving platform by aligning its body axis, or longitudinal axis, with the line of sight between the quadrotor and target in the first approach. This method is termed as the body pursuit guidance (BPG) in the literature and it dictates the quadrotor to fly just upon the target. In the second method, the motion of the quadrotor is planned in accordance with the linear homing guidance (LHG) law. In this approach, the quadrotor is driven towards a predicted intercept point with the target rather than a direct chase of the target [32]. As the second significant contribution of the present study, a two-stage control system is proposed such that it realizes the commands produced by the motion planning algorithm based on the selected guidance law by maintaining one of the rotational motions of the quadrotor fixed. In this scheme, the translational motion of the quadrotor is fully controlled along all three perpendicular axes by means of an outer loop (primary stage) according to the guidance commands in the form of linear velocity components while the control of its rotational motion about the rest two axes is carried out within an inner loop (secondary stage) whose reference, or desired, inputs are generated by the controller of the outer loop. Here, one of the angular position variables is specified at a certain value and thus a regulator-based control is applied for the control of this variable. Afterwards, the performance of the suggested approach is tried to be demonstrated by means of the computer simulations performed on the MATLAB SIMULINK environment by utilizing the constructed guidance and control models and numerical values consistent with the relevant system parameters [40; 5]. Eventually, it is shown that the motion planning of a quadrotor can be well made by a properly-selected guidance law towards moving land targets.

2. System Definition

As depicted in Fig. 1, the quadrotor is equipped with four identical rotors which are the rotary parts of the DC electric motors. In this configuration, the rotors are mounted at equal distances from the mass center of the quadrotor, i.e. point C, in the cross-shaped main chasis. The front and rear rotors which are enumerated to be 1 and 3 respectively have rotations in negative sense, or counter-clockwise direction, of the body fixed frame Fb whose origin is attached to point C and whose axes are represented by unit vectors $\vec{u}_i^{(b)}$ (i=1, 2, and 3) as shown in Fig. 1 while the left and right rotors with corresponding numbers 2 and 4 rotate in positive sense, or clockwise direction.

PRINT ISSN: 2149-4916 E-ISSN: 2149-9373

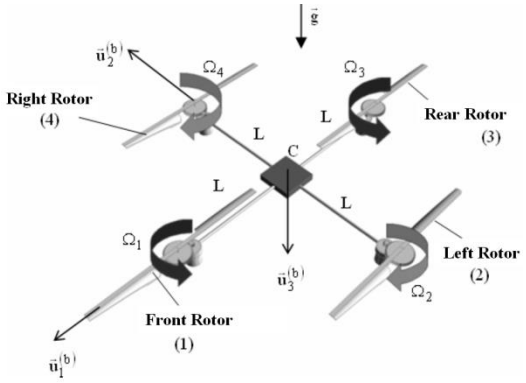

Figure 1: Schematical view of the quadrotor (Fisher, 2009).

In Fig. 1, L, Ω_j ($j=1, 2, 3, and\ 4$), and $\vec{g}$ stand for the distance between the center of rotation of each motor and point C, angular speed of the DC electric motor, used to move the propeller j, and gravity vector ($g=9.81\ m/s2$), respectively.

3. Engagement Geometry

Here, the problem is to make the quadrotor fly towards a predefined moving land platform. For this purpose, the position of the quadrotor at any instant of the engagement can be sketched along with the designated trajectory of the moving platform as shown in Fig. 2.

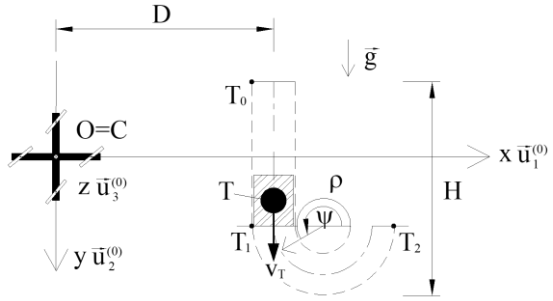

Figure 2: Engagement geometry

The explanations of the symbols indicated in Fig. 2 are given below:

$\vec{u}_i^{(0)}$: Unit vectors of the Earth-fixed reference frame denoted by F_0 ($i=1, 2, and\ 3$),
T : target point on the moving platform for the quadrotor,
T_k : points at which the shape of the trajectory of the moving platform changes ($k=0, 1, and\ 2$),
v_T : linear speed of point T on the moving platform,
ρ : radius of curvature of the trajectory of the moving platform,
ψ : rotation angle of the rounded tip portions of the trajectory of the moving platform,
H : length of the trajectory of the moving platform,
D : perpendicular distance between the origin of F_0, i.e. point O, and the midline of the section of the trajectory of the moving platform closest to this point

For a better interpretation of the relative motion considered, the engagement geometry between the quadrotor and moving land platform which is schematized in Fig. 2 can be resolved into the horizontal and vertical planes. Thus, the vertical engagement between point C and point T on the moving platform can be depicted as seen in Fig. 3. The lateral engagement geometry between points C and T can be similarly constructed by replacing the angles defined for the vertical plane with their horizontal counterparts.

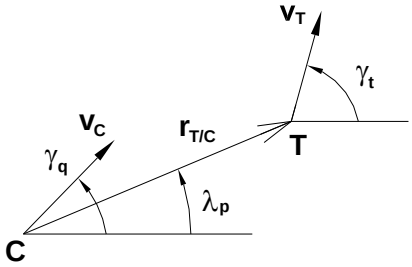

Figure 3: Vertical engagement geometry between the quadrotor and moving land platform

In Fig. 3, v_C, γ_q, $r_{T/C}$, γ_t, and λ_p show the resultant speed of point C, orientation angle of v_C from the horizontal axis, relative position of point T with respect to point C, or length of the line of sight (LOS), orientation angle of v_T from the horizontal axis, and orientation angle of $r_{T/C}$ from the horizontal axis, respectively. Here, the next equations are held for v_C, γ_t, and λ_p:

$$v_C = \sqrt{\dot{x}_C^2 + \dot{y}_C^2 + \dot{z}_C^2} \tag{1}$$

$$\gamma_t = \begin{Bmatrix} -\pi/2\ ,\ t_0 < t \le t_1 \\ (\pi/2) - \psi\ ,\ t_1 < t \le t_2 \\ \pi/2\ ,\ t > t_2 \end{Bmatrix} \tag{2}$$

$$\lambda_p = a\tan\left[(y_T - y_C)/(x_T - x_C)\right] \tag{3}$$

where x_C, y_C, and z_C indicate the position components of point C on the axes of F_0: x_T, y_T, and z_T denote the longitudinal, lateral, and vertical position components of point T: $\pi=3.14$ and for $k=0, 1$ and 2,

t_k stands for the time instant corresponding to the shape changing points of the trajectory of the moving platform.

Similarly, the orientation angle of $r_{T/C}$ from the lateral axis, i.e. λ_y, can be obtained as follows:

$$\lambda_y = a\,tan\left[\left(z_T - z_C\right)/\left(x_T - x_C\right)\right] \tag{4}$$

The final offset between points *C* and *T* at the end of the engagement, i.e. miss distance (d_{miss}), is calculated using the next formula as t_F indicates the termination instant:

$$d_{miss} = \sqrt{\Delta x^2\left(t_F\right) + \Delta y^2\left(t_F\right) + \Delta z^2\left(t_F\right)} \tag{5}$$

where;

$$\Delta x\left(t_F\right) = x_C\left(t_F\right) - x_T\left(t_F\right)$$
$$\Delta y\left(t_F\right) = y_C\left(t_F\right) - y_T\left(t_F\right)$$
$$\Delta z\left(t_F\right) = z_C\left(t_F\right) - z_T\left(t_F\right).$$

4. Dynamic Modeling of the Quadrotor

In order to design a control system which enrols to realize the path designated by the trajectory planning algorithm, it is required that the dynamic model of the quadrotor be obtained. This task can be achieved either using one of the well-known analytical principles such as Newton-Euler equations or conducting a system identification activity. Besides, it is also a preferable aproach to get a common model by gathering the information acquired by applying these two methods. On the other hand, it is almost the only way to use the analytical method for such a purpose if a physical prototype of the system under consideration is not available just as in the present study [15].

Throughout its motion, the forces acting on the quadrotor schematized in Fig. 1 are the thrust forces generated by the DC electric motors used to excite the propellers, aerodynamical reaction forces, and gravity. Here, the frictional effects on the motor bearings are not taken into account because they are at very low levels compared to other effects mentioned above. As the corresponding thrust factor is denoted by letter b, the thrust force which can be supplied by each of the identical electrical motors (F_j, *j=1, 2, 3, and 4*) can be calculated from the next expression:

$$F_j = b\,\Omega_j^2 \tag{6}$$

Expressing the gravity vector acting on the system as and making the definitions $x=x_C$, $y=y_C$, and $z=z_C$, the equations of motion of the quadrotor can be determined in the following manner using symbols ϕ, θ, and ψ which represent the angular position components of the quadrotor about the axes described by unit vector $\vec{u}_1^{(b)}$, $\vec{u}_2^{(b)}$, $\vec{u}_3^{(b)}$ i.e. roll, pitch, and yaw motions, respectively [38; 14]:

$$\ddot{\phi} = -\frac{L\,K_\phi}{J_x}\dot{\phi} + \left(\frac{J_y - J_z}{J_x}\right)\dot{\psi}\,\dot{\theta} + \frac{J_v}{J_x}\dot{\theta}\left(\Omega_1 - \Omega_2 + \Omega_3 - \Omega_4\right) + \frac{L\,b}{J_x}\left(\Omega_2^2 - \Omega_4^2\right) \tag{7}$$

$$\ddot{\theta} = -\frac{L\,K_\theta}{J_y}\dot{\theta} + \left(\frac{J_z - J_x}{J_y}\right)\dot{\psi}\,\dot{\phi} - \frac{J_v}{J_y}\dot{\phi}\left(\Omega_1 - \Omega_2 + \Omega_3 - \Omega_4\right) + \frac{L\,b}{J_y}\left(\Omega_1^2 - \Omega_3^2\right) \tag{8}$$

$$\ddot{\psi} = -\frac{K_\psi}{J_z}\dot{\psi} + \left(\frac{J_x - J_y}{J_z}\right)\dot{\theta}\,\dot{\phi} + \frac{d}{J_z}\left(-\Omega_1^2 + \Omega_2^2 - \Omega_3^2 + \Omega_4^2\right) \tag{9}$$

$$\ddot{x} = -\frac{K_x}{m}\dot{x} + \frac{b}{m}\left(\Omega_1^2 + \Omega_2^2 + \Omega_3^2 + \Omega_4^2\right)\left[c(\psi)s(\theta)c(\phi) + s(\psi)s(\phi)\right] \tag{10}$$

$$\ddot{y} = -\frac{K_y}{m}\dot{y} + \frac{b}{m}\left(\Omega_1^2 + \Omega_2^2 + \Omega_3^2 + \Omega_4^2\right)\left[s(\psi)s(\theta)c(\phi) - c(\psi)s(\phi)\right] \tag{11}$$

$$\ddot{z} = -\frac{K_z}{m}\dot{z} - g + \frac{b}{m}\left(\Omega_1^2 + \Omega_2^2 + \Omega_3^2 + \Omega_4^2\right)c(\theta)c(\phi) \tag{12}$$

In the equations above, m denotes the total mass of the quadrotor, J_x, J_y, and J_z show the moment of inertia components of the quadrotor around the axes defined by unit vectors $\vec{u}_1^{(b)}$, $\vec{u}_2^{(b)}$ and $\vec{u}_3^{(b)}$ respectively, J_v represents the moment of inertia of each rotor about its axis of rotation, d indicates the drag factor, and K_ϕ, K_θ, K_ψ, K_x, K_y, and K_z stand for the aerodynamical moment and force components acting on the system in the roll, pitch, and yaw planes and along the longitudinal, lateral, and vertical planes, respectively. Moreover, as $\alpha=\phi$, θ and ψ, the definitions $c(\alpha) = \cos(\alpha)$ and $s(\alpha) = \sin(\alpha)$ are introduced.

The system inputs to control the quadrotor can be defined as the functions of the angular speed parameters of the DC electric motors as given below [14]:

$$u_F = b\left(\Omega_1^2 + \Omega_2^2 + \Omega_3^2 + \Omega_4^2\right)/\,m \tag{13}$$

$$u_\phi = L\,b\left(\Omega_2^2 - \Omega_4^2\right)/\,J_x \tag{14}$$

$$u_\theta = L\,b\left(\Omega_1^2 - \Omega_3^2\right)/\,J_y \tag{15}$$

$$u_\psi = d\left(-\Omega_1^2 + \Omega_2^2 - \Omega_3^2 + \Omega_4^2\right)/\,J_z \tag{16}$$

From here, the equations of motion of the quadrotor can be arranged in the following manner:

$$\ddot{\phi} = -c_\phi\,\dot{\phi} + J_{\psi\theta}\,\dot{\psi}\,\dot{\theta} + J_\theta\,\Omega_e\,\dot{\theta} + u_\phi \tag{17}$$

$$\ddot{\theta} = -c_\theta\,\dot{\theta} + J_{\psi\phi}\,\dot{\psi}\,\dot{\phi} - J_\phi\,\Omega_e\,\dot{\phi} + u_\theta \tag{18}$$

$$\ddot{\psi} = -c_\psi\,\dot{\psi} + J_{\theta\phi}\,\dot{\theta}\,\dot{\phi} + u_\psi \tag{19}$$

$$\ddot{x} = -c_x\,\dot{x} + u_x \tag{20}$$

$$\ddot{y} = -c_y\,\dot{y} + u_y \tag{21}$$

$$\ddot{z} = -c_z\,\dot{z} - g + u_z \tag{22}$$

Here, the definitions below are made:
$c_\phi = L\,K_\phi / J_x$, $c_\theta = L\,K_\theta / J_y$, $c_\psi = L\,K_\psi / J_z$,
$c_x = K_x / m$, $c_y = K_y / m$, $c_z = K_z / m$,
$J_{\psi\theta} = \left(J_y - J_z\right)/ J_x$, $J_\theta = J_v / J_x$,
$J_{\psi\phi} = \left(J_z - J_x\right)/ J_y$, $J_\phi = J_v / J_y$,
$J_{\theta\phi} = \left(J_x - J_y\right)/ J_z$,
$\Omega_e = \Omega_1 - \Omega_2 + \Omega_3 - \Omega_4$,
$u_x = \left[c(\psi)s(\theta)c(\phi) + s(\psi)s(\phi)\right]u_F$,
$u_y = \left[s(\psi)s(\theta)c(\phi) - c(\psi)s(\phi)\right]u_F$,
$u_z = c(\theta)c(\phi)u_F$.

5. Kinematics of the Moving Platform

As v_T becomes constant, x_T, y_T, and z_T are defined on changing points T_k ($k=0, 1, and\ 2$) by considering the corresponding dimensional parameters of the planned trajectory and ignoring the vertical displacements $z_T(t) = z_0$ as given below:

$$\begin{Bmatrix} x_T \\ y_T \\ z_T \end{Bmatrix} = \begin{cases} x_{T0}, y_{T0} - v_T\left(t - t_0\right), z_T = z_{T0} & , t_0 < t \le t_1 \\ x_{T1} + \rho\left[cos(\psi)+1\right], y_{T1} - \rho\,sin(\psi), z_T = z_{T1} & , t_1 < t < t_2 \\ x_{T2}, y_{T2} + v_T\left(t - t_2\right), z_T = z_{T2} & , t > t_2 \end{cases} \tag{23}$$

As x_{Tk}, y_{Tk}, z_{Tk}, and tk represent the longitudinal, lateral, and vertical position components of point C at location Tk, and time parameter, respectively, the values of x_{Tk}, y_{Tk}, and z_{Tk} are listed below with the rotation angles at those points (ψ_k):

$x_{T0}=D$, $y_{T0}=(H/2)-\rho$, $z_{T0}=z_0$, $\psi_0=\pi$ rad; $x_{T1}=D$, $y_{T1}=\rho-(H/2)$, $z_{T1}=z_0$, $\psi_1=\pi$ rad; $x_{T2}=D+2\rho$, $y_{T2}=\rho-(H/2)$, $z_{T2}=z_0$, and $\psi_2=0$.

$t_1 = t_0 + \left(\left|y_{T1} - y_{T0}\right| / v_T\right)$ and $t_2 = t_1 + \left(\pi\,\rho / v_T\right)$ the parameter ψ in Eq. (23) can be calculated as a function of time (t) using the next equality for a specific t_0 value:

$$\psi = \begin{cases} \pi\ , t_0 < t \le t_1 \\ \pi - \left[v_T\left(t - t_1\right)/\,\rho\right]\ , t_1 < t \le t_2 \\ 0\ , t > t_2 \end{cases} \tag{24}$$

6. Motion Planning of the Quadrotor

In this study, the aerial motion of the quadrotor under consideration is planned according to the guidance concept towards a moving land platform. In this configuration, it is assumed that the state information of the platform is instantaneously acquired by means of a camera mounted on the main chassis of the quadrotor and this information is quantized by processing it using specific algorithms so as to compute the position and speed of the moving platform. Then, guidance commands are calculated using the position and velocity information of the quadrotor itself which is measured by the gyros and accelerometers on its main chasis and the obtained target data so as to shape the motion of the quadrotor.

When the guidance of an object is considered towards a specified moving point, the first way coming into the mind is to keep the orientation of the object throughout the motion in a manner where its longitudinal axis always indicates the point. In this extent, the BPG law can be considered as the first candidate guidance law. As the quadrotor is aimed at being oriented directly to the moving land platform with this approach at each instant of the engagement, the longitudinal axis of the quadrotor, i.e. axis indicated by unit vector $\vec{u}_1^{(b)}$ is tried to be kept coincident with LOS [32]. Hence, the guidance commands can be generated according to the following formulas in the lateral and vertical planes, respectively:

$$\psi_q^c = \lambda_y \tag{25}$$

$$\theta_q^c = \lambda_p \tag{26}$$

where ψ_q^c and θ_q^c stand for the guidance commands to the yaw and pitch angles of the quadrotor, respectively.

On the other hand, it becomes possible to use the same control system of the quadrotor with both the BPG and LHG laws by calculating corresponding commands to the lateral and vertical flight path angle components of the quadrotor, i.e. η_q^c and γ_q^c. Hence, the relevant guidance commands can be determined using the angle of attack (α) and side-slip angle (β) definitions in the following manner [19]:

$$\eta_q^c = \psi_q^c + \left[\beta / \cos\left(\theta_q^c\right)\right] \tag{27}$$

$$\gamma_q^c = \theta_q^c - \alpha \tag{28}$$

Here, $\beta = a\sin(v/v_C)$ and $\alpha = a\tan(w/u)$ as u, v, and w denote the components of v_C along the axes defined by unit vectors $\vec{u}_1^{(b)}$, $\vec{u}_2^{(b)}$, and $\vec{u}_3^{(b)}$, respectively. Regarding F_b is reached from F_0 according to the yaw, pitch, and roll (3-2-1) rotation sequence, u, v, and w can be calculated in terms of the position components of the mass center of the quadrotor in F_0 and rotation angles as follows [32]:

$$u = \left[\dot{x}\cos(\psi) + \dot{y}\sin(\psi)\right]\cos(\theta) - \dot{z}\sin(\theta) \tag{29}$$

$$v = \left[\dot{x}\cos(\psi) + \dot{y}\sin(\psi)\right]\sin(\theta)\sin(\phi) - \left[\dot{x}\sin(\psi) - \dot{y}\cos(\psi)\right]\cos(\phi) + \dot{z}\cos(\theta)\sin(\phi) \tag{30}$$

$$w = \left[\dot{x}\cos(\psi) + \dot{y}\sin(\psi)\right]\sin(\theta)\cos(\phi) + \left[\dot{x}\sin(\psi) - \dot{y}\cos(\psi)\right]\sin(\phi) + \dot{z}\cos(\theta)\cos(\phi) \tag{31}$$

In order to diminish the total engagement time and hence the power consumption of the quadrotor, the LHG law is proposed as an alternative to the BPG law. Unlike the direct orientation strategy of the BPG law, the guided object is driven to a predicted intercept point with the target point in the LHG strategy. As the object, target, and predicted intercept point form a triangular shape called the collision triangle whose dimensions are continuously updated during the engagement, the objective is first to put and then to keep the velocity vector of the object on the fictitious line connecting the object and predicted intercept point on the collision triangle [32].

In this approach, in order for point C on the quadrotor to catch point T on the platform, the guidance commands can be derived in terms of the orientation angles of v_C from the lateral and vertical axes (and) in the following manner [31]:

$$\eta_q^c = a\tan\left[\left(v_{Ty}\,\Delta t - \Delta y\right)/\left(v_{Tx}\,\Delta t - \Delta x\right)\right] \tag{32}$$

$$\gamma_q^c = a\tan\left[\frac{\Delta z - v_{Tz}\,\Delta t}{\left(v_{Tx}\,\Delta t - \Delta x\right)\cos\left(\eta_q^c\right) + \left(v_{Ty}\,\Delta t - \Delta y\right)\sin\left(\eta_q^c\right)}\right] \tag{33}$$

where
$\Delta x = x_C - x_T$, $\Delta y = y_C - y_T$ and $\Delta z = z_C - z_T$

In Eqs. (32) and (33), the components of the linear velocity vector of point T whose amplitude is v_T, i.e. v_{Tx}, v_{Ty}, and v_{Tz}, are defined in the following equations:

$$v_{Tx} = v_T\cos\left(\gamma_t\right) \tag{34}$$

$$v_{Ty} = v_T\sin\left(\gamma_t\right) \tag{35}$$

$$v_{Tz} = 0 \tag{36}$$

Furthermore, the remaining time duration till the end of the engagement, i.e. t, is formulated below [31]:

$$\Delta t = \left[\sqrt{\sigma^2 + \left(v_C^2 - v_T^2\right)\Delta r^2} - \sigma\right]/\left(v_C^2 - v_T^2\right) \tag{37}$$

where
$\sigma = v_{Tx}\,\Delta x + v_{Ty}\,\Delta y + v_{Tz}\,\Delta z$
$\Delta r^2 = \Delta x^2 + \Delta y^2 + \Delta z^2$.

Since the control inputs of the designed control system are linear velocity components, the guidance commands given in Eqs. (32) and (33) should be expressed in terms of the linear velocity parameters for realization. This transformation can be made by writing the velocity vector of point C with amplitude v_C in terms of its components on F_0 as follows:

$$\bar{\boldsymbol{x}}_{\boldsymbol{pd}} = \boldsymbol{v_C}\begin{bmatrix}\boldsymbol{\cos\left(\eta_q^c\right)\cos\left(\gamma_q^c\right)}\\ \boldsymbol{\sin\left(\eta_q^c\right)\cos\left(\gamma_q^c\right)}\\ \boldsymbol{-\sin\left(\gamma_q^c\right)}\end{bmatrix} \tag{38}$$

Here, Eq. (38) results in an algebraic loop because v_C is obtained from command. In order to overcome this difficulty, it will be convenient to consider a nonzero v_C value at the initiation of the engagement. Actually, this is fair reasonable assumption because

the quadrotor has to be provided by an initial nonzero thrust in order to start its flight. For this reason, the speed of point *C* is gradually raised to a value specified as the initiation speed of the engagement within a certain time interval (t_e) and the engagement between the quadrotor and the moving target is started after that time.

7. Control System of the Quadrotor

The control system which will be designed for the quadrotor should not only have a satisfactory tracking capability for the guidance commands but it should also be able to supress the undesired and diverting effects of the disturbances on the quadrotor such as wind and gust. That means, the robustness of the control system should also be guaranteed. For this purpose, the simplest way is to consider a proven control algorithm as done here while a more sophisticated robust control method can be utilized to satisfy more stringent conditions [15; 4]. As explained above, the guidance commands are generated in terms of the linear velocity components of the mass center of the quadrotors. In order to convert these commands into physical motion, the control system should bring the linear velocity components of the quadrotor to the desired, i.e. reference, values dictated by the guidance commands. At the same time, the angular position, i.e. orientation, requirement of the quadrotor arising at a result of the proposed control process should also be satisfied. For this purpose, a two-stage control scheme is constructed such that the outer loop makes the linear velocity control in accordance with the guidance commands whilst the inner loop satisfies the orientation requirement resulted during the linear velocity control. In this sense, since the linear velocity components are desired to be attained the values dictated by the guidance law without any error, it is reasonable to consider an action which supresses the steady state error in the outer control system. In other words, the integral action should be added to the control law of the outer loop. On the other hand, there is no necessity to completely remove the steady state errors in the inner loop because the probable errors in the inner control system can be nullified by the outer control loop.

Here, Eqs. (20) through (22) can be used in the design of the linear velocity control system called "the primary control system". These expressions can be rearranged in the state space form by assigning the columns of the state variables and inputs of the system to be $\bar{x}_p = \begin{bmatrix} \dot{x} & \dot{y} & \dot{z} \end{bmatrix}^T$ and $\bar{u}_p = \begin{bmatrix} u_x & u_y & u_z \end{bmatrix}^T$, respectively as letter "*T*" indicates the transpose operation as follows:

$$\dot{\bar{x}}_p = -\hat{C}_p \, \bar{x}_p + \bar{u}_p \tag{39}$$

where

$$\hat{\boldsymbol{C}}_p = \begin{bmatrix} \boldsymbol{c_x} & \boldsymbol{0} & \boldsymbol{0} \\ \boldsymbol{0} & \boldsymbol{c_y} & \boldsymbol{0} \\ \boldsymbol{0} & \boldsymbol{0} & \boldsymbol{c_z} \end{bmatrix}$$

The control law of the primary control system including an integral action utilized to nullify the steady state errors can be designed as per the computed torque method with PI (proportional plus integral) action as:

$$\bar{\boldsymbol{u}}_p = \dot{\bar{\boldsymbol{x}}}_{pd} + \hat{\boldsymbol{C}}_p \, \bar{\boldsymbol{x}}_p + \hat{\boldsymbol{K}}_{pp} \, \bar{\boldsymbol{e}}_p + \hat{\boldsymbol{K}}_{pi} \int \bar{\boldsymbol{e}}_p \, \boldsymbol{dt} \tag{40}$$

In the expression above, $\bar{\boldsymbol{x}}_{pd}$, $\hat{\boldsymbol{K}}_{pp}$, $\hat{\boldsymbol{K}}_{pi}$ and $\bar{\boldsymbol{e}}_p$ denote the desired input column, proportional gain matrix, integral gain matrix, and error column for the primary control system, respectively, and the definition $\bar{\boldsymbol{e}}_p = \bar{\boldsymbol{x}}_{pd} - \bar{\boldsymbol{x}}_p$ is introduced.

Substituting Eq. (40) into Eq. (39), the error dynamics of the primary control system is obtained as below:

$$\ddot{\bar{\boldsymbol{e}}}_p + \hat{\boldsymbol{K}}_{pp} \, \dot{\bar{\boldsymbol{e}}}_p + \hat{\boldsymbol{K}}_{pi} \, \bar{\boldsymbol{e}}_p = \bar{\boldsymbol{0}} \tag{41}$$

As ω_{pi} and ζ_{pi} represent the desired bandwidth and damping ratio of the i_{th} state variable (*i=1, 2, and 3*) of the primary control system, respectively, the error dynamics of a second order ideal system with three degrees of freedom can be described using the forthcoming expression [31]:

$$\ddot{\bar{\boldsymbol{e}}}_p + \hat{\boldsymbol{D}}_p \, \dot{\bar{\boldsymbol{e}}}_p + \hat{\boldsymbol{W}}_p \, \bar{\boldsymbol{e}}_p = \bar{\boldsymbol{0}} \tag{42}$$

where

$$\hat{\boldsymbol{D}}_p = \begin{bmatrix} \boldsymbol{2\zeta_{p1}\,\omega_{p1}} & \boldsymbol{0} & \boldsymbol{0} \\ \boldsymbol{0} & \boldsymbol{2\zeta_{p2}\,\omega_{p2}} & \boldsymbol{0} \\ \boldsymbol{0} & \boldsymbol{0} & \boldsymbol{2\zeta_{p3}\,\omega_{p3}} \end{bmatrix}$$

and

$$\hat{\boldsymbol{W}}_p = \begin{bmatrix} \boldsymbol{\omega_{p1}^2} & \boldsymbol{0} & \boldsymbol{0} \\ \boldsymbol{0} & \boldsymbol{\omega_{p2}^2} & \boldsymbol{0} \\ \boldsymbol{0} & \boldsymbol{0} & \boldsymbol{\omega_{p3}^2} \end{bmatrix}$$

Matching Eqs. (41) and (42), the gain matrices are found for the primary control system as follows:

$$\hat{\boldsymbol{K}}_{pp} = \hat{\boldsymbol{D}}_p \tag{43}$$

$$\hat{\boldsymbol{K}}_{pi} = \hat{\boldsymbol{W}}_p \tag{44}$$

As the corresponding columns of the state variables and inputs of the system are shown to be $\bar{\boldsymbol{x}}_s = \begin{bmatrix} \boldsymbol{\phi} & \boldsymbol{\theta} & \boldsymbol{\psi} \end{bmatrix}^T$ and $\bar{\boldsymbol{u}}_s = \begin{bmatrix} \boldsymbol{u}_{\boldsymbol{\phi}} & \boldsymbol{u}_{\boldsymbol{\theta}} & \boldsymbol{u}_{\boldsymbol{\psi}} \end{bmatrix}^T$, the matrix equality below is reached via Eqs. (17) through (19) for the orientation, or attitude, control system termed as "the secondary control system":

$$\ddot{\bar{\boldsymbol{x}}}_s = \bar{\boldsymbol{b}}_s + \bar{\boldsymbol{u}}_s \tag{45}$$

where

$$\bar{\boldsymbol{b}}_s = \begin{bmatrix} -\boldsymbol{c}_{\boldsymbol{\phi}}\,\dot{\boldsymbol{\phi}} + \left(\boldsymbol{J}_{\boldsymbol{\psi\theta}}\,\dot{\boldsymbol{\psi}} + \boldsymbol{J}_{\boldsymbol{\theta}}\,\Omega_e\right)\dot{\boldsymbol{\theta}} \\ -\boldsymbol{c}_{\boldsymbol{\theta}}\,\dot{\boldsymbol{\theta}} + \left(\boldsymbol{J}_{\boldsymbol{\psi\phi}}\,\dot{\boldsymbol{\psi}} - \boldsymbol{J}_{\boldsymbol{\phi}}\,\Omega_e\right)\dot{\boldsymbol{\phi}} \\ -\boldsymbol{c}_{\boldsymbol{\psi}}\,\dot{\boldsymbol{\psi}} + \boldsymbol{J}_{\boldsymbol{\theta\phi}}\,\dot{\boldsymbol{\theta}}\,\dot{\boldsymbol{\phi}} \end{bmatrix}$$

In a similar manner, the control law can be written according to the computed torque method with PD (proportional plus derivative) action for the secondary control system as follows:

$$\bar{\boldsymbol{u}}_s = \ddot{\bar{\boldsymbol{x}}}_{sd} - \bar{\boldsymbol{b}}_s + \hat{\boldsymbol{K}}_{sp}\,\bar{\boldsymbol{e}}_s + \hat{\boldsymbol{K}}_{sd}\,\dot{\bar{\boldsymbol{e}}}_s \tag{46}$$

Here, $\bar{\boldsymbol{x}}_{sd}$, $\hat{\boldsymbol{K}}_{sp}$, $\hat{\boldsymbol{K}}_{sd}$, and $\bar{\boldsymbol{e}}_s$ stand for the desired input column, proportional gain matrix, derivative gain matrix, and error column for the secondary control system, respectively. Also, the definition $\bar{\boldsymbol{e}}_s = \bar{\boldsymbol{x}}_{sd} - \bar{\boldsymbol{x}}_s$ is made for the error term.

In the proposed entire control scheme, the desired values of ϕ and θ are calculated using u_x, u_y, and u_z inputs along with the parameter u_F by regarding the definitions within Eqs. (17) through (22). In other words, the reference inputs, or commands, to ϕ and θ are generated by the outer loop. On the other hand, the remaining angular position variable ψ is adjusted to be a constant value. That means its reference value is set as a fixed quantity. In this sense, the desired value of ψ is then specified to be zero as the decision on keeping the quadrotor with no angular motion in the yaw plane [38; 42]. Inserting Eq. (46) into Eq. (45), the error dynamics of the secondary control system is obtained as:

$$\ddot{\bar{\boldsymbol{e}}}_s + \hat{\boldsymbol{K}}_{sd}\,\dot{\bar{\boldsymbol{e}}}_s + \hat{\boldsymbol{K}}_{sp}\,\bar{\boldsymbol{e}}_s = \bar{\boldsymbol{0}} \tag{47}$$

As ω_{si} and ζ_{si} denote the desired bandwidth and damping ratio of the i_{th} state variable ($i=1, 2, and\ 3$) of the secondary control system, the error dynamics of a second order ideal system with three degrees of freedom can be described using the following equation [31]:

$$\ddot{\bar{\boldsymbol{e}}}_s + \hat{\boldsymbol{D}}_s\,\dot{\bar{\boldsymbol{e}}}_s + \hat{\boldsymbol{W}}_s\,\bar{\boldsymbol{e}}_s = \bar{\boldsymbol{0}} \tag{48}$$

where

$$\hat{\boldsymbol{D}}_s = \begin{bmatrix} 2\boldsymbol{\zeta}_{s1}\,\boldsymbol{\omega}_{s1} & \boldsymbol{0} & \boldsymbol{0} \\ \boldsymbol{0} & 2\boldsymbol{\zeta}_{s2}\,\boldsymbol{\omega}_{s2} & \boldsymbol{0} \\ \boldsymbol{0} & \boldsymbol{0} & 2\boldsymbol{\zeta}_{s3}\,\boldsymbol{\omega}_{s3} \end{bmatrix}$$

and

$$\hat{\boldsymbol{W}}_s = \begin{bmatrix} \boldsymbol{\omega}_{s1}^2 & \boldsymbol{0} & \boldsymbol{0} \\ \boldsymbol{0} & \boldsymbol{\omega}_{s2}^2 & \boldsymbol{0} \\ \boldsymbol{0} & \boldsymbol{0} & \boldsymbol{\omega}_{s3}^2 \end{bmatrix}$$

Equating expressions numbered as (47) and (48) to each other yields the gain matrices of the secondary control system as shown below:

$$\hat{\boldsymbol{K}}_{sp} = \hat{\boldsymbol{W}}_s \tag{49}$$

$$\hat{\boldsymbol{K}}_{sd} = \hat{\boldsymbol{D}}_s \tag{50}$$

For the sake of maintaining the stability, the gain matrices are continuously updated for both the primary and secondary control systems throughout the planned motion using the state information of target acquired by the camera on the main chassis of the quadrotor and the data collected by the sensors of the quadrotor own.

8. Computer Simulations

In order to see the effectiveness of the proposed guidance-based motion planning algorithm, the simulation models are constructed by gathering the models obtained above. Here, the expressions describing the plant dynamics, engagement geometry, and guidance rule are used with their original nonlinear forms in order to reflect the actual behaviour of the entire physical system as realistic as possible in the computer simulation environment. Also, in order

to be able to make a fair comparison, the same control system is utilized for both the guidance algorithms based on the PNG and LHG laws. From here, the computer simulations are carried out by considering the numerical values given in Table 1 as *i=1*, *2*, and *3*. The numerical values are decided in accordance with a standard commercial quadrotor.

Table 1: Numerical values used in the simulations

Parameter	Numerical Value	Parameter	Numerical Value
L	0.25 m	K_ϕ, K_θ, and K_ψ	0.012 N·s/m
b	5×10-5 N·s^2	ω_{pi}	31. 4 rad/s (=5 Hz)
d	1×10-6 N·m·s^2	ω_{si}	94. 2 rad/s (=15 Hz)
m	2 kg	ζ_{pi} and ζ_{si}	0.707
J_x and J_y	0.2 kg·m^2	H	50 m
J_z	0.3 kg·m^2	ρ	15 m
J_v	1×10-3 kg·m^2	D	50 m
K_x, K_y, and K_z	0.01 N·s/m	Solver Step	1 ms

In the engagement geometries in which point *C* is assumed to be coincident with the origin of F_0, i.e. $x_{C0}=y_{C0}=z_{C0}=0$, at the beginning, the initial values of point T_k on the moving platform are adjusted to be $x_{T0}=50m$, $y_{T0}=50m$, and $z_{T0}=2m$ for all the situations considered. *A* ramp-type angular speed inputs are applied to point *C* which is initially stationary so as to make it attain the specified initial engagement speed ($v_{Pe}=0.1m/s$) at $t_e=10ms$. Assuming that random disturbing torques and forces whose maximum amplitudes are *50Nm* and *100N* act on the angular and linear dynamics of the quadrotor, respectively, the simulations are terminated once the miss distance drops down *0.1m.* Although it is ignored in the design phase of the control system, the gravity (g) is added to the vertical dynamics of the quadrotor. In the simulations, ODE5 (Dormand-Prince) type solver is utilized with the constant step as in Table 1.

Having performed the computer simulations in MATLAB SIMULINK environment by taking the limits of the components of the linear and angular velocity vectors of the quadrotor to be *15m/s* and *5rad/s*, respectively, the results in Table 2 are attained for both the BPG and LHG cases. The engagement geometries of the sample configurations 5 and 6 are plotted in Fig. 4 through Fig. 13 as well as the yaw, pitch, and roll speed components. In these plots, solid lines stand for point *T* on the moving target whereas the dashed lines indicate point *C* of the quadrotor.

Table 2: Results attained from the considered simulation configurations

Conf. No.	Moving Platform Speed (km/h)	Moving Platform Speed (m/s)	Guidance Law	Engagement Duration (s)	Maximum Speed of the Mass Center of the Quad rotor (m/s)
1	10	2.778	BPG	6.516	25.981
2			LHG	5.098	37.180
3	20	5.556	BPG	10.182	25.981
4			LHG	5.306	26.323
5	30	8.333	BPG	10.215	25.981
6			LHG	8.041	25.779

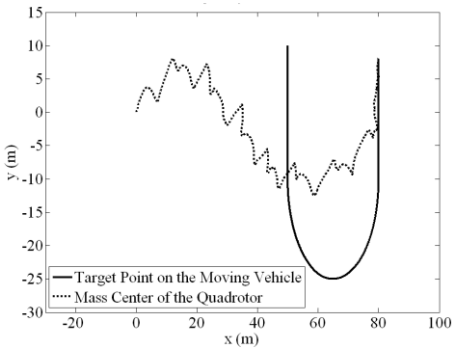

Figure 4: Horizontal engagement for configuration 5

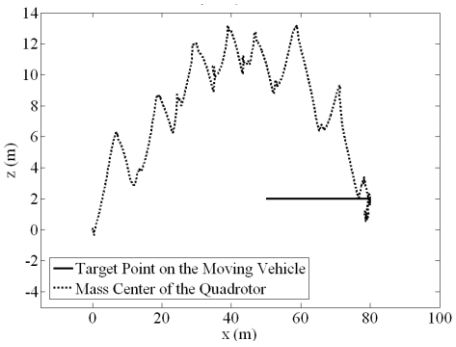

Figure 5: Vertical engagement for configuration 5

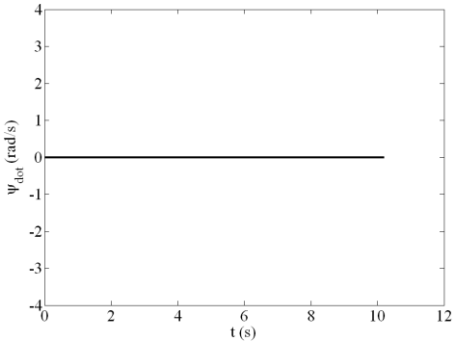

Figure 6: Change of the yaw speed component in time for configuration 5

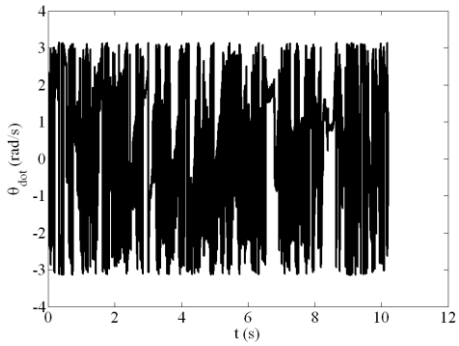

Figure 7: Change of the pitch speed component in time for configuration 5

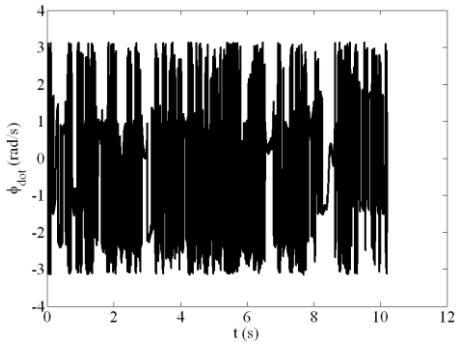

Figure 8: Change of the roll speed component in time for configuration 5

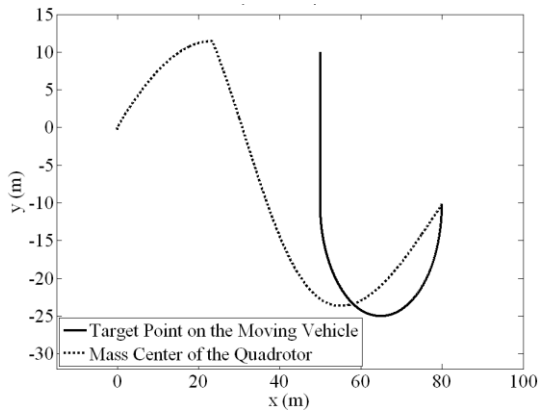

Figure 9: Horizontal engagement for configuration 6

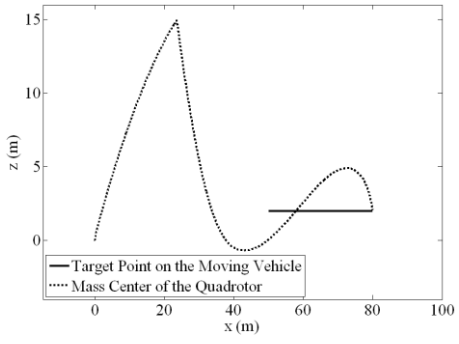

Figure 10: Vertical engagement for configuration 6

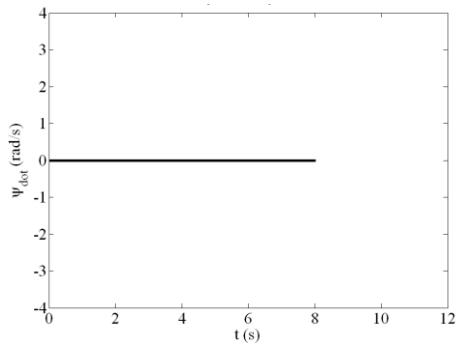

Figure 11: Change of the yaw speed component in time for configuration 6

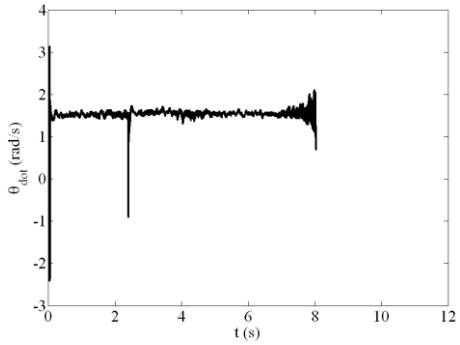

Figure 12: Change of the pitch speed component in time for configuration 6

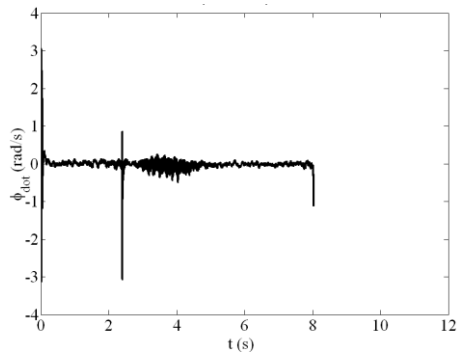

Figure 13: Change of the roll speed component in time for configuration 6

9. Discussion

In this study, the guidance approach is applied to an engagement problem between an aerial system and a moving land platform successfully. In this sense, the BPG and LHG laws are compared for the performance criteria including the engagement duration and maximum speed of the mass center of the quadrotor. When the results attained in the computer simulations as submitted in Table 2 are examined, it is observed that LHG law yields smaller engagement durations than the BPG law under all conditions. This fact can

also be seen when the relevant trajectory of the mass center of the quadrotor is traced for the engagement geometries in both the horizontal and vertical planes. On the other hand, the BPG law seems to be superior in the sense of the maximum speed of the mass center to LHG.

Considering the change of the pitch and roll speed components in time, the LHG results in smoother response with considerably lower amplitudes. Unsurprisingly, the yaw speed component remains to be zero for both the guidance laws because the yaw angle of the quadrotor is specified to be zero in all of the situations simulated.

10. Conclusion

Guidance-based motion planning algorithms can be applied to quadrotors aimed at reaching moving land platforms to decrease the engagement time and power consumption. In this sense, the LHG guidance law which aims at driving the mass center of the quadrotor towards a predicted collision point with the target point appears to be a better and viable solution for the quidance problem of the quadrotor than the BPG law which dictates a direct pursuit of the target.

References

[1] Abbasi, E., Mahjoob, M. J. and Yazdanpanah, R. 2013: Controlling of quadrotor UAV using a fuzzy system for tuning the PID gains in hovering mode. Proceedings of the Advances in Database and Data Mining Conference (ADDM-2013), İstanbul, Turkey.

[2] Altuğ, E., Ostrowski, J. P. and Mahony, R. 2002: Control of a quadrotor helicopter using visual feedback. Proceeding of the 2002 IEEE International Conference on Robotics and Automation, Washington DC, USA.

[3] Asl, H. J. and Bolandi, H. 2014: Robust vision-based control of an underactuated flying robot tracking a moving target. Transactions of the Institute of Measurement and Control, 36, 3, 411-424.

[4] Bouabdallah, S. and Siegwart, R. 2007: Full control of a quadrotor. Proceedings of the Intelligent Robots and Systems Conference-2007 (IROS 2007), San Diego, CA, USA.

[5] Bresciani, T. 2008: Modelling, Identification and Control of a Quadrotor Helicopter. MSc Thesis, Lund University, Sweden.

[6] Capello, E., Guglieri, G. and Quagliotti, F. 2011: Modeling and simulation of a small quad-rotor UAV.

[7] Aerotecnica Missili and Spazio, The Journal of Aerospace Science, Technology and Systems, 89, 21, 90-99.

[8] Castellanos, J. F. G., Guzmán, J. J. T., Durand, S., Marchand, N., Muňoz, J. U. A, and Díaz, V. R. G. 2014: Attitude stabilization of a quadrotor by means of event-triggered nonlinear control. Journal of Intelligent Robot Systems, 73, 123-135.

[9] Cowling, I. D., Yakimenko, O. A., Whidborne, J. F. and Cooke, A. K. 2007: A prototype of an autonomous controller for a quadrotor UAV. Proceedings of the European Control Conference 2007 (ECC'07), Kos, Greece.

[10] Cutler, M. J. 2012: Design and Control of an Autonomous Variable-Pitch Quadrotor Helicopter. MSc Thesis, Massachusetts Institute of Technology, Boston, MA, USA.

[11] Dougherty, J., Lee, D. and Lee, T. 2014: Laser-based guidance of a quadrotor UAV for precise landing on an inclined surface. Proceedings of the American Control Conference 2014, Portland, OR, USA.

[12] Dydek, Z. T., Annaswamy, A. M. and Lavretsky, E. 2013: Adaptive control of quadrotor UAVs: A design trade study with flight evaluations. IEEE Transactions on Control Systems Technology, 21, 4, 1400-1406.

[13] Ellis, D., Brady, T., Olson, I. and Li, Y. 2013: Autonomous Quadrotor for the 2012 International Aerial Robot Competition. Technical Report, M.S.E. Aerospace Engineering.

[14] Erginer, B. and Altuğ, E. 2007: Fuzzy control of a helicopter with four rotors (in Turkish). Proceedings of the Automatic Control Turkish National Committee, Automatic Control National Meeting-2007 (TOK'07), Sabancı University, İstanbul, Turkey.

[15] Fernandes, S. I. B. 2011: Guidance and Trajectory Following of an Autonomous Vision-

Guided Micro Quadrotor. MSc Thesis, Technical University of Lisbon, Lisbon, Portugal.

[16] Fisher, M. 2009: Attitude Stabilisation of a Quadrotor Aircraft. Faculty of Engineering and Physical Systems, Central Queensland University, Australia.

[17] Fowers, S. G. 2008: Stabilization and Control of a Quad-rotor Micro-UAV Using Vision Sensors. MSc Thesis, Brigham Young University, USA.

[18] Ghadiok, V., Goldin, J. and Ren, W. 2012: On the design and development of attitude stabilization, vision-based navigation, and aerial gripping for a low-cost quadrotor. Autonomous Robots, 33, 1-2, 41-68.

[19] Härkegård, O. 2001: Flight Control Design Using Backstepping. MSc Thesis, Linköping University, Sweden.

[20] Hehn, M. and D'Andrea, R. 2011: Quadrocopter trajectory generation and control. Proceedings of the 18th World Congress of the International Federation of Automatic Control (IFAC 2011), Milano, Italy.

[21]Hérissé, B., Hamel, T., Mahony, R. and Russotto, F. X. 2012: Landing a VTOL unmanned aerial vehicle on a moving platform using optical flow. IEEE Transactions on Robotics, 28, 1, 77-89.

[22] Hoffmann, G. M., Huang, H., Waslander, S. L. and Tomlin, C. J. 2007: Quadrotor helicopter flight dynamics and control: theory and experiment. Proceedings of the AIAA Guidance, Navigation and Control Conference and Exhibit, South Carolina, USA.

[23] Huo, X., Huo, M. and Karimi, H. R. 2014: Attitude stabilization control of a quadrotor UAV by using backstepping approach. Mathematical Problems in Engineering, Hindawi Publishing Corporation, 2014, 1-9.

[24] Kendoul, F. 2012: A Survey of Advances in Guidance, Navigation and Control of Unmanned Rotorcraft Systems. Technical Report, Australian Research Centre for Aerospace Automation (ARCAA), Australia.

[25] Kıvrak, A. Ö. 2006: Design of Control Systems for a Quadrotor Flight Vehicle Equipped with Inertial Sensors. MSc Thesis, Atılım University, Turkey.

[26] Lee, K. U., Park, J. B. and Choi, Y. H. 2014: Adaptive backstepping hovering control for a quadrotor with unknown parameters. Journal of Institute of Control, Robotics and Systems, 20, 10, 1002-1007.

[27] Li, W., Zhang, T. and Kühlenz, K. 2011: A vision-guided autonomous quadrotor in an air-ground multi- robot system. Proceedings of the 2011 IEEE International Conference on Robotics and Automation (ICRA), Shanghai, China.

[28] Liu, H., Bai, Y., Lu, G., Shi, Z. and Zhong, Y. 2014: Robust tracking control of a quadrotor helicopter. Journal of Intelligent Robot Systems, 75, 595-608.

[29] Miller, K. 2008: Path Tracking Control for Quadrotor Helicopters. Technical Report.

[30] Morel, Y. and Leonessa, A. 2006: Direct adaptive tracking control of quadrotor aerial vehicles. Proceedings of the 2006 Florida Conference on Recent Advances in Robotics (FCRAR 2006), Miami, Florida, USA.

[31] Özkan, B. 2016: Guidance and control of a planar robot manipulator used in an assembly line. Transactions of the Institute of Measurement and Control, OnlineFirst Publication, 1-11.

[32] Özkan, B. 2005: Dynamic Modeling, Guidance, and Control of Homing Missiles. Ph.D Dissertation, Middle East Technical University, Ankara, Turkey.

[33] Richter, C., Bry, A. and Roy, N. 2013: Polynomial trajectory planning for quadrotor flight. Proceedings of the International Conference on Robotics.

[34] Rodriguez, H. R., Vega, V. P., Orta, A. S. and Salazar, O. G. 2014: Robust backstepping control based on integral sliding modes for tracking of quadrotors. Journal of Intelligent Robot Systems, 73, 51-66.

[35] Stevanovic, S., Kasac, J. and Stepanic, J. 2012: Robust tracking control of a quadrotor helicopter without velocity measurement. Proceedings of the 23rd International DAAAM Symposium, Vienna, Austria.

[36] Tsay, T. S. 2014: Guidance and control laws for quadrotor UAV. WSEAS Transactions on Systems and Control, 9, 1, 606-613.

[37] Tsay, T. S. 2012: Model based automatic regulation process for guidance and control of quadrotor UAV. Journal of Aeronautics, Astronautics, and Aviation, 46, 4, 271-279.

[38] Voos, H. and Nourghassemi, B. 2009: Nonlinear control of stabilized flight and landing for quadrotor UAVs. Proceedings of the 24th Annual Meeting of the European Institute for Applied Research, IAR'2009, Zielona, Góra, Poland.

[39] Wang, W., Ma, H., Xia, M., Weng, L. and Ye, X. 2013: Attitude and altitude controller design for quad-rotor type MAVs. Mathematical Problems in Engineering, Hindawi Publishing Corporation, 2013, 1-9.

[40] Xu, R. and Özgüner, Ü. 2008: Sliding mode control of a class of underactuated systems. Automatica, Elsevier, 44, 233-241.

[41] Zarchan, P. 1994: Tactical and Strategic Missile Guidance. Vol. 157, Progress in Aeronautics and Astronautics, AIAA, Washington DC, USA, Chapters: 1-3.

[42] Zhang, D., Qi, H., Wu, X., Xie, Y. and Xu, J. 2014: The quadrotor dynamic modeling and ındoor target tracking control method. Mathematical Problems in Engineering, Hindawi Publishing Corporation, 2014, 1-9.

Bülent ÖZKAN

Bülent ÖZKAN was born in 1974 in Taşköprü. He was graduated from the mechanical engineering department of Gazi University in 1991. Afterwards, he took the MSc and PhD degrees from Middle East Technical University in mechanical engineering in 1999 and 2005, respectively. He has worked in TÜBİTAK SAGE since 2000. His research interests are on system dynamics, guidance and control, robotics, dynamics of machinery, and mechanisms. He is married and has a son.